PHILOSOPHICAL MAGAZINE A, 2001, VOL. 81, NO. 5, 1387–1407

Atomistic study of non-Schmid effects in the plastic yielding of bcc metals

K. ITO

Department of Materials Science and Engineering, Kyoto University, Sakyo-ku, Kyoto 606-8501, Japan

and V. VITEK†

Department of Materials Science and Engineering, University of Pennsylvania, Philadelphia, Pennsylvania 19104, USA

[*Received 13 July 2000 and accepted in revised form 11 December 2000*]

ABSTRACT

In this paper we investigate by computer modelling, using many-body central force potentials, the response of the core of $\frac{1}{2}$[111] screw dislocations in bcc transition metals to externally applied stresses. The objective is to identify those components of the applied stress tensor which play the main role in the breakdown of the Schmid law and to establish the dependence of the critical stress needed for dislocation motion upon these stress components. This development lays the ground for constitutive relations that reflect correctly the non-Schmid character of plastic flow in bcc metals that are needed in continuum approaches to plasticity of these materials. First, we investigate the effect of pure shear stress acting parallel to the Burgers vector. This study involves calculation of the critical resolved shear stress (CRSS) for various orientations of the maximum resolved shear stress plane. The results show the dependence on the sense of shearing, exhibit the so-called twinning–antitwinning asymmetry and reveal quantitatively the overall deviation from the Schmid law. The next step is investigation of the effect of tensile and compressive stresses for a number of differently oriented tension or compression axes. These calculations demonstrate that shear stresses parallel to the Burgers vector are not sufficient to explain the variation in the CRSS with the orientation of the loading axis and suggest that other components of the stress tensor are affecting the dislocation behaviour. Finally, a combined effect of the shear stresses parallel and perpendicular to the Burgers vector is investigated. The resultant dependence of the CRSS on the shear stress perpendicular to the Burgers vector explains the orientation dependence found in the tension and compression studies. The present atomistic calculations establish that gliding of the $\frac{1}{2}$[111] screw dislocation in bcc metals depends on shear stresses both parallel and perpendicular to the Burgers vector that act not only in the slip plane but all three {110} and also {112} planes of the [111] zone. The results of these calculations determine the functional dependence of the CRSS on these shear stresses.

§1. INTRODUCTION

Plastic flow of bcc metals displays many features that are typical signatures of dislocation core effects: unusual deformation modes and slip geometries,

† Email: vitek@lrsm.upenn.edu

Philosophical Magazine A ISSN 0141–8610 print/ISSN 1460-6992 online © 2001 Taylor & Francis Ltd
http://www.tandf.co.uk/journals
DOI: 10.1080/01418610110033885

rapid increase in the flow stress with decreasing temperature that indicates a high-lattice-friction (Peierls) stress, strong dependence of the flow stress on crystal orientation and, most prominently, a breakdown of the Schmid law. This law states that glide on a given slip system, defined by a slip plane and direction of slip, commences when the resolved shear stress on that system, the Schmid stress, reaches a critical value (Schmid and Boas 1935). This implicitly assumes that other components of the stress tensor than shear in the slip plane in the slip direction play no role in the deformation process and that the critical stress is independent of the sense of shearing. The stress tensor components regarded as insignificant are

(i) shear stresses in the direction of slip acting in crystallographic planes other than the slip plane and
(ii) stress tensor components that cannot drive the glide in the slip direction, for example shear stresses in the direction perpendicular to the slip direction.

These assumptions are valid in metals with close-packed crystal structures for which the Schmid law was originally established. However, the observed dependences of the yield stress on the orientation of the tension or compression axes and the markedly different critical shear stresses for loading in tension and compression respectively demonstrate that they are not valid in bcc metals (for reviews see Christian (1970, 1983), Vitek (1975, 1985), Kubin (1982), Duesbery (1989) and Duesbery and Vitek (1998)). In fact there is no crystallographic reason why shearing in opposite direction along $\langle 111 \rangle$ should be equivalent since $\{111\}$ planes are not mirror planes in the bcc lattice; this is in contrast with the $\langle 110 \rangle$ slip direction of fcc crystals since $\{110\}$ planes are mirror planes and this symmetry then guarantees the equivalence of the two senses of slip. At this point it is also interesting to note that already the early deformation experiments of Taylor and Elam (1926) and Taylor (1928) established firm evidence of deficiencies in the Schmid law in α-Fe and β-brass, both of which crystallize in the bcc structures.

A very important link between the fundamental investigation of the plastic properties of materials and engineering applications is study of plastically deforming crystals made in the framework of the finite-strain continuum theory (Rice 1971, Hill and Rice, 1972, Asaro 1983, Bassani 1994). The overwhelming majority of such studies have assumed the Schmid-type constitutive behaviour and, consequently, they principally apply to materials with close-packed crystal structures, and in particular fcc metals. One exception is the work of Qin and Bassani (1992a, b) and Vitek *et al.* (1996) on $L1_2$ compounds which included non-Schmid behaviour into the continuum framework. In order to advance the finite-strain continuum approach to bcc metals the constitutive behaviour has to reflect correctly the breakdown of the Schmid law and the primary purpose of this paper is to lay the ground for establishment of such constitutive relations.

Many experimental and theoretical studies performed in the last 40 years have unequivocally established that the core structure of $\frac{1}{2}\langle 111 \rangle$ screw dislocations controls these aspects of the plastic behaviour of bcc metals. A number of comprehensive reviews that deal with this topic are available (Christian 1970, 1983, Vitek 1975, 1985, Kubin 1982, Duesbery 1989, Taylor 1992, Duesbery and Vitek 1998). The most prominent characteristic of the core of $\frac{1}{2}\langle 111 \rangle$ screw dislocations is its spreading into several non-parallel planes of the $\langle 111 \rangle$ zone. This possibility was first recognized by Hirsch (1960) and it became the guiding idea of both experimental and theoretical studies of the plastic behaviour of bcc metals. Michael Duesbery participated in the

seminal experimental studies that established the special significance of screw dislocations in bcc metals (Foxall *et al.* 1967, Duesbery and Foxall 1969), contributed very significantly to the development of the theoretical description of the glide of such dislocations (Duesbery and Hirsch 1968, Duesbery 1969) and became one of the leaders in the early atomistic computer simulations that established the nonplanar character of the core of $\frac{1}{2}\langle 111\rangle$ screw dislocations (Vitek *et al.* 1970, Basinski *et al.* 1971, 1972, Duesbery *et al.* 1973). In general, the core of screw dislocations in bcc metals is always spread into three $\{110\}$ planes of the $\langle 111\rangle$ zone and two types of spreading, with threefold and sixfold symmetry respectively have been found (Duesbery 1989, Duesbery and Vitek 1998).

In this paper, which is a follow-up on the recent study by Duesbery and Vitek (1998), we present results of atomistic calculations that focus on the complex response of the core of $\frac{1}{2}[111]$ screw dislocations to externally applied stresses. The calculations were made using central-force many-body potentials for Mo and Ta (Ackland and Thetford 1987) which typify the two distinct forms of core structure found in previous calculations (Duesbery and Vitek 1998). First, we investigate the effect of pure shear stress acting parallel to the Burgers vector; this stress is always resolved in the plane where it is maximum—the maximum resolved shear stress plane (MRSSP). The study then involves calculation of the critical resolved shear stress (CRSS) for various orientations of the MRSSP. The results demonstrate the dependence of the CRSS on the sense of shearing, reveal the so-called twinning–antitwinning asymmetry (Christian 1983, Duesbery 1989) and exhibit the dependence of the CRSS on the orientation of the MRSSP that does not follow the Schmid law.

The next step in this study is investigation of the effect of tensile and compressive stresses on the motion of screw dislocation. This has been done for a number of differently oriented tension or compression axes chosen such that several of them always correspond to the same MRSSP. These calculations demonstrate that differences in shear stresses parallel to the Burgers vector are insufficient to explain the variation in the CRSS with the orientation of the loading axis. This implies that other components of the stress tensor are affecting the dislocation behaviour. Following Duesbery's (1984a, b) pioneering study of the influence of non-glide stresses on the motion of dislocations in bcc metals, we focus on shear stresses in the direction perpendicular to the Burgers vectors. A combined effect of the shear stresses parallel and perpendicular to the Burgers vector has then been investigated. The ensuing dependence of the CRSS on the shear stress perpendicular to the Burgers vector explains the orientation dependence of the CRSS found in the calculations investigating the effect of tensile and compressive stresses. Hence, the present atomistic calculations establish that gliding of the $\frac{1}{2}[111]$ screw dislocation in bcc metals depends on shear stresses both parallel and perpendicular to the Burgers vector that act not only in the slip plane but in all three $\{110\}$ and $\{112\}$ planes of the [111] zone. The results of these calculations determine the functional dependence of the CRSS on these shear stresses.

§ 2. Method of calculation and representation of results

The atomistic calculations presented in this paper have all been made using many-body central force potentials of the Finnis–Sinclair (1984) type for Mo and Ta (Ackland and Thetford 1987). A molecular statics method of minimizing the energy of the system by gradually moving the particles so as to attain zero forces

on each atom was employed in the relaxation calculations, similarly to the previous calculations (Duesbery and Vitek 1998). Periodic boundary conditions were applied in the direction of the dislocation line with the period equal to the Burgers vector $\frac{1}{2}[111]$. Thus an infinite straight screw dislocation at 0 K was considered. The block of atoms in the form of a parallelepiped was divided into an inner part in which the atoms were relaxed, and an outer part in which the atoms were assigned displacements evaluated in accordance with the anisotropic elastic field of the dislocation studied (Hirth and Lothe 1982). The total numbers of atoms both in the block and in the inner part were adjusted during the calculation so that in the relaxed configuration the force on any atom would be smaller than 10^{-3} eV Å^{-1}, unless the dislocation began to move. 2000–3000 atoms were usually present in the inner block. When applying the external stress the elastic displacement field corresponding to this stress was evaluated using anisotropic elasticity and superimposed on the dislocation displacement field for the atoms in both the inner and the outer regions. The relaxation then proceeded as in the non-stressed case. When evaluating the CRSS, we always started with the fully relaxed core structure; then the applied stress was increased incrementally and full relaxation carried out at every step until the dislocation started to move. This stress level was then identified with the critical stress needed for the dislocation glide at 0 K.

The most important feature of dislocation cores is possible dissociation into partial dislocations involving metastable stacking faults. In bcc metals no such stacking faults exist (Vitek 1975, Christian 1983, Duesbery 1989) but the concept can still be useful although fractional dislocations and 'generalized stacking faults', introduced by Duesbery *et al.* (1973), have to be considered. In this context the most significant theoretical constructs are γ surfaces (Vitek 1968, 1975, Duesbery 1989) which represent energies of generalized stacking faults formed by displacing two parts of a crystal relative to each other along a cut typically identified with a low-index crystallographic plane. In bcc metals the most important are γ surfaces for {110} and {112} planes. Their relation to the dislocation core structure was discussed in detail by Duesbery and Vitek (1998). In the context of investigation of dislocation motion under the effect of external stresses an important quantity is the ideal shear strength of the material representing an upper limit of the critical stress needed for slip at 0 K. This quantity can be easily determined using the γ surface since it is the maximum value of the derivative of this surface with respect to the displacement in a chosen direction in the corresponding crystallographic plane. Using the previously calculated γ surfaces, the ideal shear strengths for shearing in the {110} plane in $\langle 111 \rangle$ direction in Mo and Ta are $0.11C_{44}$ and $0.15C_{44}$ respectively, where C_{44} is the elastic modulus. For shearing in the $\langle 111 \rangle$ direction along the {112} plane the ideal shear strengths for Mo and Ta are $0.12C_{44}$ and $0.18C_{44}$ respectively. As explained in §4.1, for the $\langle 111 \rangle$ direction, shears in the positive and the negative sense are not equivalent. The ideal shear strengths are, indeed, different for the two different senses of shearing but, unlike in the case of dislocation motion (see §4.1), this difference is only marginal.

The core structures are presented in this paper using the standard method of differential displacements (see the reviews by Duesbery (1989), Vitek (1992) and Duesbery and Vitek (1998)). In these displays the atomic arrangement is shown in the projection perpendicular to the direction of the dislocation line ([111]) and circles represent atoms within one period without distinguishing their positions in three successive (111) planes. The chosen component of the relative displacement of the

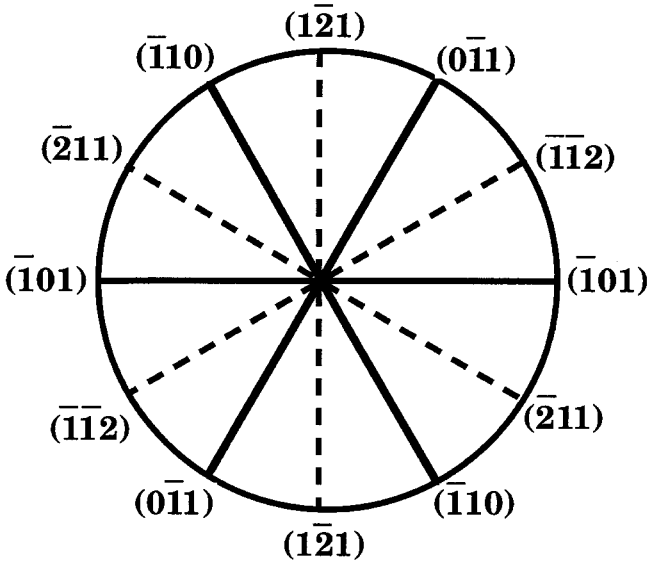

Figure 1. [111] stereographic projection showing orientations of all {110} and {112} planes belonging to the [111] zone.

neighbouring atoms produced by the dislocation is depicted as an arrow between them. Components both parallel (screw) and perpendicular (edge) to the total Burgers vector are presented, albeit separately. The lengths of the arrows are proportional to the magnitudes of these components. In the case of screw displacements the arrows, which indicate out-of-plane displacements, are always drawn along the line connecting neighbouring atoms and their length is normalized such that it is equal to the separation of these atoms in the projection when the magnitude of their relative displacement is equal to $|\frac{1}{6}[111]|$. For the edge displacements the arrows are centred between the corresponding atoms and their directions indicate the directions of the relative displacement of these atoms perpendicular to the Burgers vector (and dislocation line), that is in the plane of the figure. The lengths of the arrows are proportional to the magnitudes of the edge displacements but, since these are generally much smaller than the screw displacements, the largest length is always chosen so as to make them well discernible. To facilitate the interpretation of the displays of differential displacements the orientations of all the {110} and {112} planes belonging to the [111] zone are shown in figure 1.

§ 3. Structure of the core of $\frac{1}{2}[111]$ screw dislocations

The core structures calculated using the potential for Mo are shown in figures 2 (*a*) and (*b*) in terms of screw and edge differential displacements respectively. The core is spread asymmetrically into the planes $(\bar{1}01), (0\bar{1}1)$ and $(\bar{1}10)$ that belong to the [111] zone; the orientation of the crystal planes is defined in figure 1. This core structure is not invariant with respect of the $[10\bar{1}]$ diad, a symmetry operation of the bcc lattice. Following the so-called Neumann's (1885) principle which states that 'Any kind of symmetry which is possessed by the crystal structure of the material is also possessed by any physical property of the material', another energetically equivalent configuration related by this symmetry operation must exist. This alter-

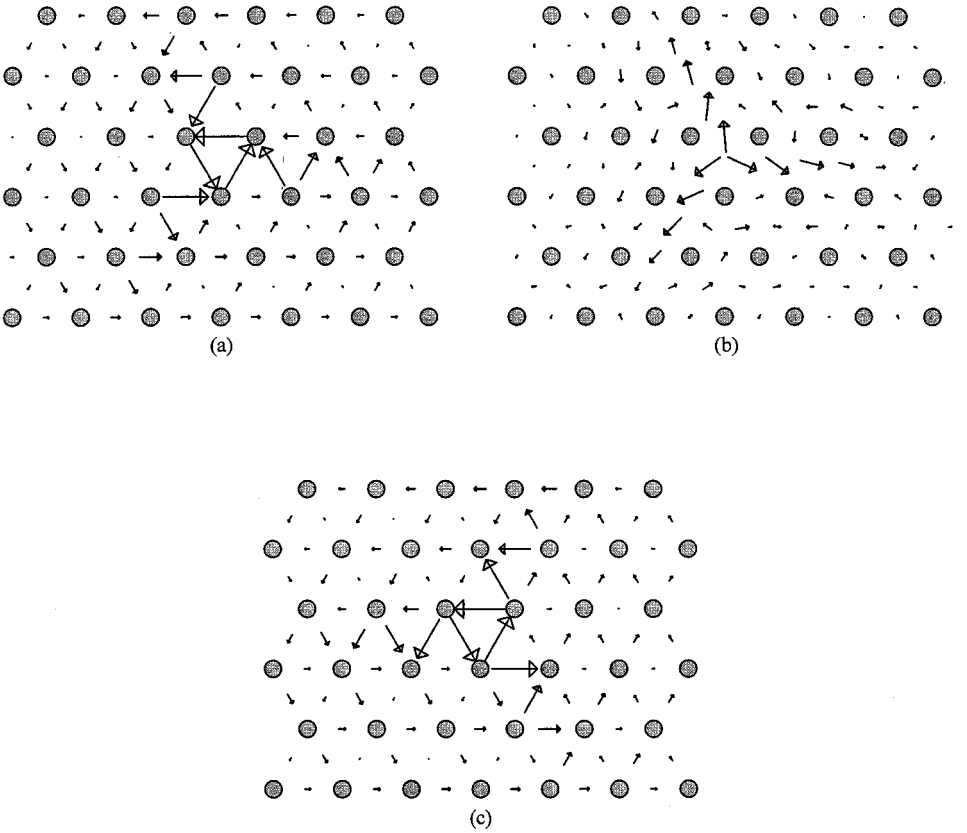

Figure 2. The core structure of the $\frac{1}{2}[111]$ screw dislocation in Mo in terms of (*a*) screw and (*b*) edge differential displacements. (*c*) Alternative core configurations related by the $[10\bar{1}]$ diad to that shown in (*a*).

native configuration of the screw dislocation core is shown in figure 2(*c*). Hence, the core of this type is degenerate as it exists in two symmetry-related but otherwise identical variants.

However, it does not mean that one or the other variant of the core is maintained along the entire length of a screw dislocation. As first suggested by Kroupa (1963), the two variants may alternate along the dislocation line and the regions separating them may be associated with jogs, kinks, local core constrictions and other irregularities. Furthermore, at finite temperatures, transitions between the two variants that possess the same energy may occur relatively easily with the help of thermal activation. In general, we can expect that, at a given applied stress, one of the variants will be easier to move. This is shown in § 4.1 for the case of pure shear. However, if both variants are present along the dislocation line and/or may transform one into another, the variant requiring a lower stress will determine the critical stress for the glide of screw dislocations.

The degenerate core structure, shown in figure 2, was found in earlier calculations employing generic pair potentials (Vitek *et al.* 1970, Vitek 1975, Vitek and Duesbery, 1982, Duesbery 1989), pair potentials for alkali metals (Basinski *et al.* 1971, 1972, 1981) as well as in the recent calculations (Xu and Moriarty 1996) using

multi-ion interatomic potentials derived from first-principles modified generalized pseudopotential theory (MGPT) (Moriarty 1990a, b), This core structure can be perceived as a generalized splitting into three fractional dislocations with screw components $\frac{1}{6}[111]$ (Duesbery *et al.* 1973, Duesbery and Vitek 1998). As seen from figure 2 (*b*), there are also significant edge displacements in the core and these can be interpreted in terms of edge components of the three fractional dislocations.

The core structure found when using the potential for Ta is shown in figure 3. In contrast with the core shown in figure 2 it is non-degenerate since it is invariant to the $[10\bar{1}]$ diad. It is spread symmetrically across the planes $(\bar{1}01)$, $(0\bar{1}1)$ and $(\bar{1}10)$ and can be regarded as splitting into six fractional dislocations with screw components $\frac{1}{12}[111]$ (Duesbery *et al.* 1973, Duesbery and Vitek 1998). As seen from figure 3 (*b*) there are also edge displacements in the core and these can be again interpreted in terms of edge components of the fractional dislocations. This type of the core was previously found in studies employing pair potentials (Minami *et al.* 1972, 1974, Kuramoto *et al.* 1974,), an approximate tight-binding technique (Masuda and Sato 1978, Sato and Masuda 1981) and recently in *ab initio* calculations for both Mo and Ta (IsmailBeigi and Arias 2000, Woodward and Rao 2001). However, in all these calculations the completeness of relaxations is uncertain either because of limitation of the relaxation to the direction of the Burgers vector only, or owing to the necessity to impose three-dimensional periodic boundary conditions. It has been shown by Duesbery and Vitek (1998) in calculations free of such restrictions that for the Finnis–Sinclair type central-force potentials (Ackland and Thetford 1987) the degenerate core is found for VIB and the non-degenerate core for VB transition metals. Using the concept of γ surfaces this was rationalized in terms of similar cohesive energies but different elastic moduli in these two groups of transition metals (Duesbery and Vitek 1998). However, the recent calculations employing MGPT potentials for Ta suggest a degenerate core but less widely spread than in Mo. Furthermore, the degeneracy disappears when the lattice is slightly expanded while degenerate core spreading increases with increasing hydrostatic compression (Yang *et al.* 2001). Evidently, the differences between different transition elements cannot be unambiguously established in the framework of central forces since the d electrons dominate bonding in these materials (Friedel 1969, Pettifor 1995). Nevertheless, the two core structures shown in figures 2 and 3 typify the two distinct nonplanar core configurations that may occur in bcc metals even if they cannot be

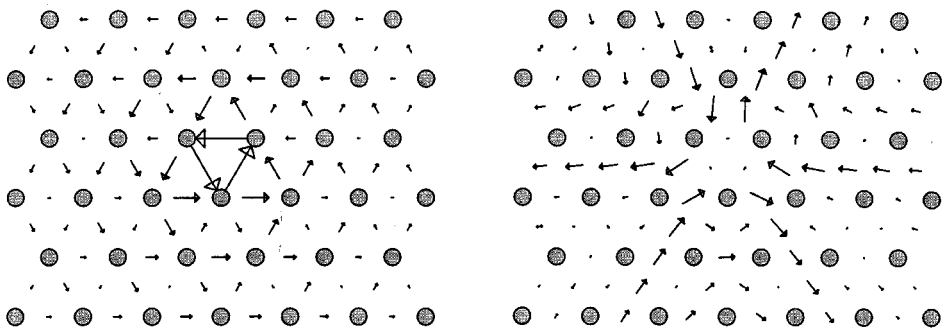

Figure 3. The core structure of the $\frac{1}{2}[111]$ screw dislocation in Ta in terms of (*a*) screw and (*b*) edge differential displacements.

firmly associated with Mo and Ta respectively. In the following the response of these two types of core to external loading is investigated.

§ 4. Effect of externally applied stresses

4.1. *Pure shear stress in the [111] direction*

First we consider external loading corresponding to the application of a shear stress parallel to the Burgers vector, that is the stress that exerts the Peach-Koehler force on the $\frac{1}{2}[111]$ screw dislocation. The goal is to investigate the dependence of the stress at which the dislocation starts to move on the orientation of the MRSSP. In this paper the shear stress acting in the [111] direction, denoted in the following as $\tau_{\parallel}$, is always given as the stress in the MRSSP, and its value when the dislocation starts to move is referred to as the CRSS. In the computer simulations the stress was applied using the procedure described in § 2.

The orientation of the MRSSP is defined by the angle χ which it makes with one of the {110} planes of the [111] zone. This representation of the orientation of the MRSSP has been commonly used in earlier theoretical and experimental studies (Christian 1983, Duesbery 1989). In this paper we always measure the angle χ with respect to the $(\bar{1}01)$ plane as shown in figure 4. Owing to the crystal symmetry it is sufficient to consider $-30^\circ \leqslant \chi \leqslant 30^\circ$; the sign of χ is defined in figure 4. However, it should be noted that orientations corresponding to positive and negative angles χ are not equivalent. In general, for an orientation χ the shear in the [111] direction is equivalent to the shear in the $[\bar{1}\bar{1}\bar{1}]$ direction for the orientation $-\chi$ but, for a given χ, shears along [111] and $[\bar{1}\bar{1}\bar{1}]$ are not generally equivalent because the (111) plane is not a mirror plane in the bcc lattice. This asymmetry, related to the sense of shearing, has usually been described in terms of the twinning–antitwinning asymmetry of shear on {112} planes. However, it applies to all planes of a $\langle 111 \rangle$ zone except planes of the {110} type for which the $\langle 101 \rangle$ type diad symmetry operation assures the symmetry with respect to the sense of shearing. Since the notion of the twinning-antitwinning asymmetry is a common terminology (for example Vitek (1975), Christian (1983), Duesbery (1989) and Duesbery and Vitek (1998)) we shall employ it in this paper. If an applied stress induces the Peach–Koehler force on the $\frac{1}{2}[111]$ dislocation that points to the right in figure 4, the $(\bar{1}\bar{1}2)$ plane is sheared

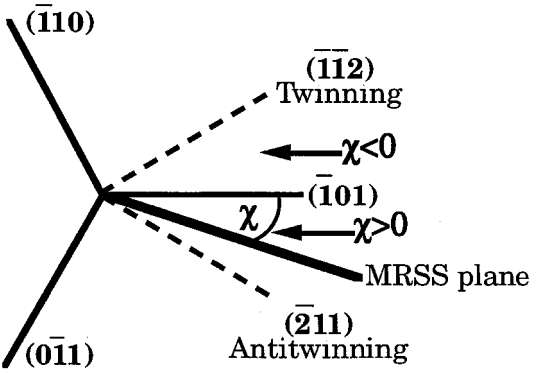

Figure 4. Definiton of the angle χ describing the orientation of the MRSSP relative to the $(\bar{1}01)$ plane.

in the twinning sense and the $(\bar{2}11)$ plane in the antitwinning sense. Hence, we call the orientations of the MRSSP for which $-30^\circ \leqslant \chi < 0^\circ$ orientations of the twinning shear and those corresponding to $0^\circ < \chi \leqslant 30^\circ$ orientations of the antitwinning shear. When the sign of the applied stress changes, the twinning and antitwinning orientations interchange.

Calculated dependences of the CRSS on χ are shown in figures 5 (*a*) and (*b*) for Mo and Ta respectively. In the case of Mo the calculations were made for two symmetry-related configurations of the core, shown in figures 2 (*a*) and (*c*) respectively. It is seen that the CRSS is always higher for the configuration shown in figure 2 (*c*), except for $\chi = \pm 30^\circ$ when the two configurations become equivalent. As discussed in § 3, we may assume that both configurations of the core are always present and the configuration which moves more easily determines the CRSS for dislocation glide since the other may always transform into it. Hence, we only need to consider the core configuration of figure 2 (*a*) for this orientation of the applied stress.

For all values of χ, except $+30^\circ$, the dislocation moved along the $(\bar{1}01)$ plane. For $\chi = +30^\circ$ it moved on average along the $(\bar{2}11)$ plane, but the path was com-

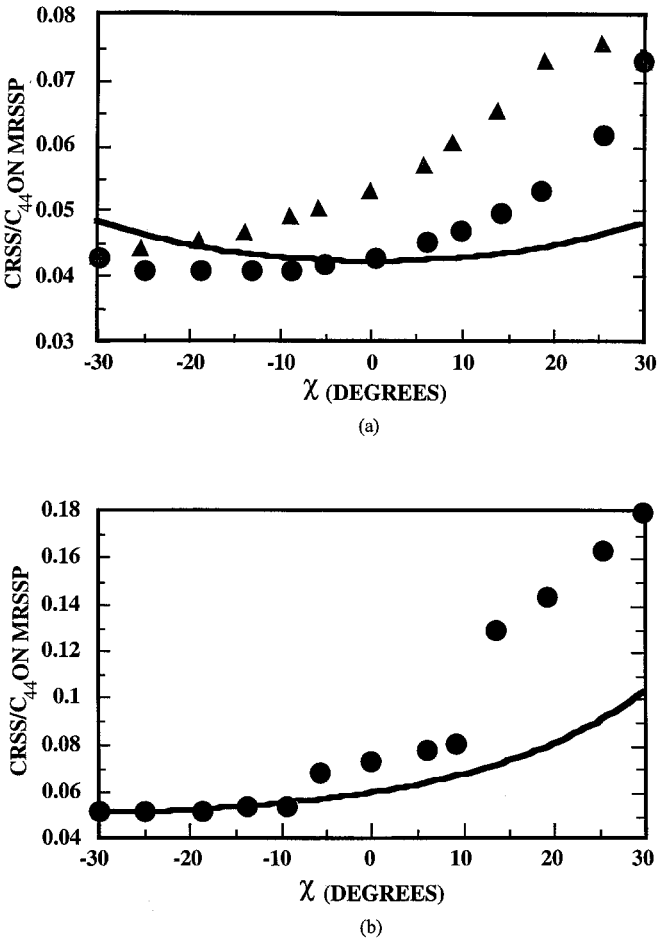

Figure 5. Calculated dependences of the CRSS on χ for (*a*) Mo and (*b*) Ta.

posed of segments of $(\bar{1}01)$ and $(\bar{1}10)$ planes that are equivalent for this orientation. However, it should be noted that for $\chi = -30^\circ$ the $(0\bar{1}1)$ and $(\bar{1}01)$ planes are also equivalent and thus the movement along the $(\bar{1}01)$ plane is a consequence of the relaxation routine and not a preference for this plane. The CRSS versus χ dependence clearly demonstrates that the Schmid law is not valid. According to the Schmid law the dependence of the CRSS on χ should have the form $1/\cos\chi$, shown as a full curve in figure 5(*a*), since $(\bar{1}01)$ is the slip plane. The reason for the non-Schmid behaviour is that prior to the dislocation motion the nonplanar core is altered under the influence of the applied stress and these modifications are dependent on the orientation of the MRSSP. This is seen in figures 6(*a*) and (*b*) where the displacement maps of the dislocation core are shown for $\chi = -30^\circ$ and $\chi = +30^\circ$ respectively, for stress levels somewhat lower than the corresponding CRSS. In the former case the core spreading into $(0\bar{1}1)$ is constricted, spreading into $(\bar{1}01)$ is extended and spreading into $(\bar{1}10)$ is almost unaffected. In the latter case the spreading into the $(\bar{1}10)$ plane is constricted while spreading into the $(\bar{1}01)$ plane is extended. At the same time the part of the core that was originally spread into the $(0\bar{1}1)$ plane extends into the $(\bar{1}10)$ plane so that the eventual motion of the dislocation proceeds by equal steps along $(\bar{1}01)$ and $(\bar{1}10)$ planes. These changes in the core structure occurring before the dislocation starts to move are induced by shear stresses acting in the [111] direction in all three {110} planes containing this direction and can be interpreted as repositioning of the corresponding fractional dislocations under the effect of these shear stresses.

In the case of Ta the dislocation moved along the $(\bar{1}\bar{1}2)$ plane, inducing shearing in the twinning sense, for all values of χ less than $+30^\circ$. A typical example of the core transformation that occurs prior to the onset of the motion is shown in figures 7(*a*) and (*b*) which display the displacement maps of the dislocation cores for $\chi = 0^\circ$ ($(\bar{1}01)$ is the MRSSP) and magnitudes of the applied stress of $0.04C_{44}$ and $0.05C_{44}$ respectively. In figure 7(*a*) the centre of the core is still in the original position, although the displacements are distributed asymmetrically, with large displacements spread in the $[\bar{1}10]$ direction away from the centre. In figure 7(*b*) the centre of the dislocation is displaced away from its original position and the changes that occurred in the core can be interpreted in two equivalent ways. First, they can be

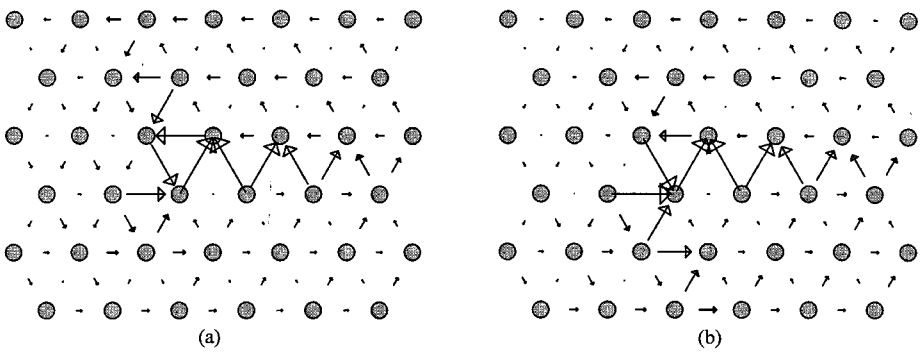

Figure 6. The displacement maps of the dislocation core in Mo for (*a*) $\chi = -30^\circ$ and (*b*) $\chi = +30^\circ$, for stress levels somewhat lower than the corresponding CRSS.

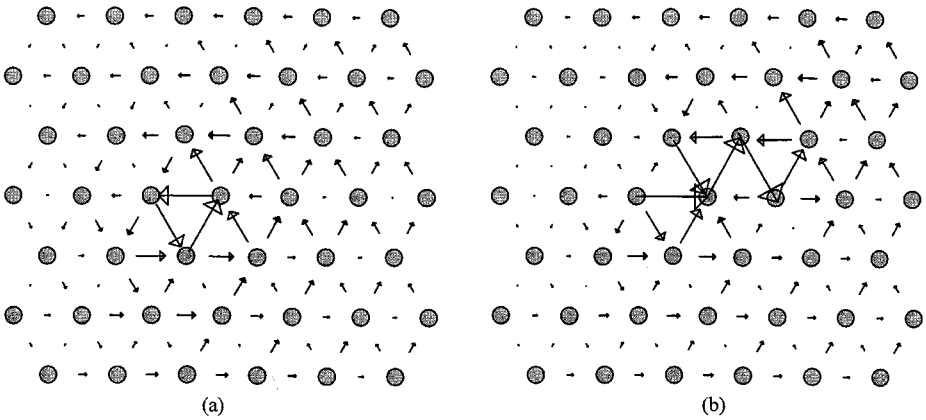

Figure 7. The displacement maps of the dislocation core in Ta for $\chi = 0^\circ$ and applied stresses (*a*) $0.04C_{44}$ and (*b*) $0.05C_{44}$.

regarded as a development of a microtwin in three $(\bar{1}\bar{1}2)$ layers that eventually moves along the $(\bar{1}\bar{1}2)$ plane in steps of $[\bar{1}10]$. An alternative description is that the dislocation moves sequentially along the $(0\bar{1}1)$ and $(\bar{1}01)$ planes in steps of $\frac{1}{3}[\bar{2}11]$ and $\frac{1}{3}[\bar{1}2\bar{1}]$ respectively. This type of core transformation occurred for all MRSSP orientations with $\chi < 30^\circ$, although sharp increases in the CRSS appear for χ close to -8° and 12°. For $\chi = +30^\circ$, very complex core changes took place and the dislocations moved along $(\bar{2}11)$ plane, inducing shearing in the antitwinning sense. However, at this point the applied stress reached the ideal strength for shear on {112} planes ($0.18C_{44}$; see §2) and thus, effectively, for $\chi = +30^\circ$ the screw dislocation is completely immobile. It should be noted that shear stresses of corresponding magnitude were never attained in Mo.

The CRSS versus χ dependence (figure 5(*b*)) again shows that the Schmid law is not valid. When $(\bar{1}\bar{1}2)$ is the slip plane, then according to the Schmid law the dependence of the CRSS on χ should have the form $1/\cos(\chi + 30^\circ)$, drawn as a full curve in figure 5(*b*). This shows that the Schmid law is nearly obeyed for orientations of the MRSSP close to the $(\bar{1}\bar{1}2)$ plane, which is sheared in the twinning sense. The deviation from the Schmid law becomes discernible for $\chi > -8^\circ$ and increases rapidly as the MRSSP approaches the $(\bar{2}11)$ plane that is sheared in the antitwinning sense.

4.2. *Tension and compression*

Mechanical testing of materials is usually carried out using tensile and/or compressive loading. While only the shear stress $\tau_{\|}$ in the direction of the Burgers vector generates the Peach–Koehler force which can drive the motion of the dislocations with this Burgers vector, other components of the stress tensor are always present in tension and compression tests. These components do not produce the Peach–Koehler force on this dislocation, but they still can affect the dislocation core, and thus the CRSS and, presumably, the slip geometry. To investigate this possibility, computer simulation of the effect of tensile and compressive loading on the $\frac{1}{2}[111]$ screw dislocation was carried out for five different axes of tension and compression, which are shown in the [001] stereographic projection in figure 8. They were chosen within the standard triangle such that the corresponding MRSSPs concur with the

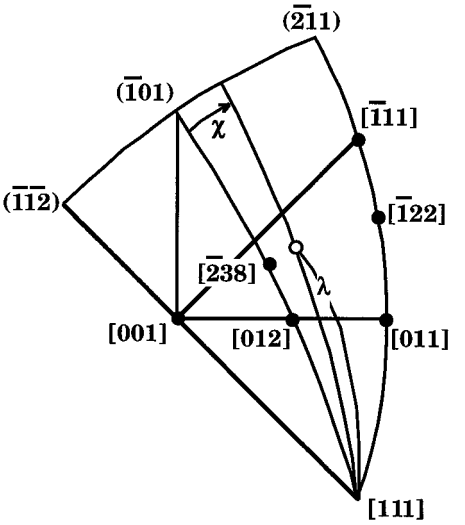

Figure 8. [001] stereographic projection showing the orientation of the five tension and compression axes used in the study of the effect of uniaxial loading.

following planes: $(\bar{1}01)$ for the axes $[\bar{2}38]$ and [012], $(\bar{1}\bar{1}2)$ for the axis [001], and $(\bar{2}11)$ for the axes $[\bar{1}11]$, $[\bar{1}22]$ and [011]. For the axis [001] the shear in the $(\bar{1}\bar{1}2)$ plane is in the twinning sense for tension and antitwinning sense for compression; for the axes $[\bar{1}11]$, $[\bar{1}22]$ and [011] the shear in the $(\bar{2}11)$ plane is in the twinning sense for compression and antitwinning sense for tension.

The results are presented in figures 9 and 10 for Mo and Ta respectively in terms of the CRSS on the MRSSP corresponding to a given tension–compression axis. For

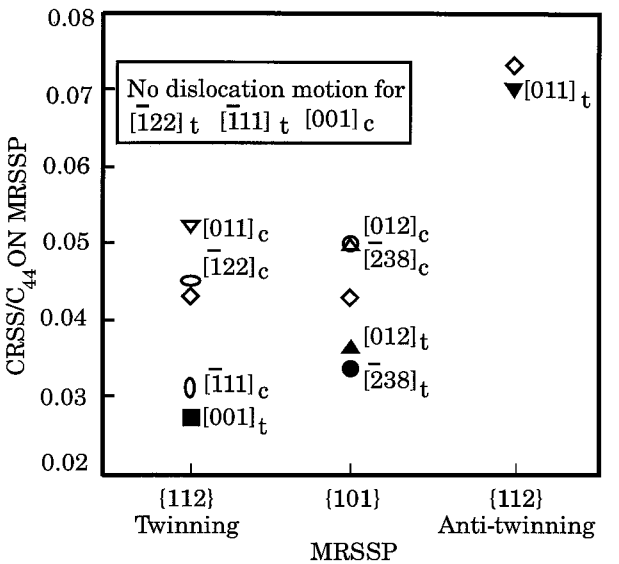

Figure 9. CRSS on the MRSSP for the $\frac{1}{2}[111]$ screw dislocation in Mo loaded in tension or compression for different orientations of the tensile or compressive axis.

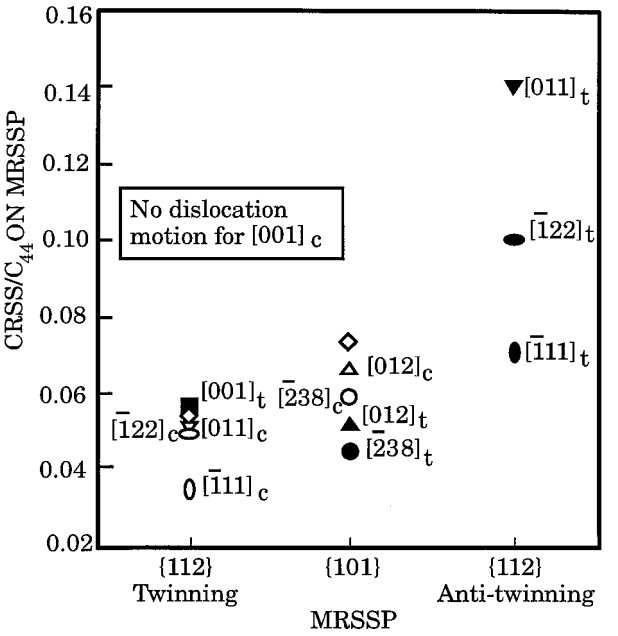

Figure 10. CRSS on the MRSSP for the $\frac{1}{2}[111]$ screw dislocation in Ta loaded in tension or compression for different orientations of the tensile or compressive axis.

{112} planes as MRSSPs the results are shown separately for shearing in the twinning and antitwinning sense so that {112} twinning means the $(\bar{1}\bar{1}2)$ plane for tension in [001] but the $(\bar{2}11)$ plane for compression in $[\bar{1}11]$, $[\bar{1}22]$ and [011] and vice versa for {112} antitwinning. If only the shear stress $\tau_{\|}$ in the direction of the Burgers vector affected the dislocation glide, then for a given orientation of the MRSSP the CRSS would be the same regardless of the orientation of the tensile or compressive axis and the only difference between tension and compression would result from the difference in the sense of shearing. The latter means that no difference between tension and compression would be seen when a {101} plane is the MRSSP and, when a {112} plane is the MRSSP, the difference would be the same as observed in the case of pure shear, related to the twinning-antitwinning asymmetry. It is seen from figures 9 and 10 that this is not the case. Thus, the results indubitably demonstrate that other stress components than the shear stress in the direction of the Burgers vector significantly influence the dislocation glide. This effect is strong for all orientation studied but is particularly so when the MRSSP is a {112} plane sheared in the antitwinning sense. In fact, in the case of Mo the resolved shear stress reached the ideal shear strength for tension in $[\bar{1}22]$ and $[\bar{1}11]$ directions and compression in the [001] direction and no dislocation motion occurred. Thus, the CRSS was very significantly increased relative to that for pure shear. In the case of Ta the same effect is observed for compression in [001] direction but, in contrast with Mo, for tension in $[\bar{1}22]$ and $[\bar{1}11]$ directions the CRSS is significantly decreased relative to that for pure shear. A smaller decrease is also found for tension in [011] direction.

In the case of Mo the dislocation always moved along the $(\bar{1}01)$ plane as in the case of pure shear. Thus the stress components other than $\tau_{\|}$ do not affect significantly the slip geometry. The situation is somewhat different in Ta. While for most

cases the plane of dislocation glide is the same as in pure shear, that is the {112} plane sheared in the twinning sense, in several cases the dislocation moved along the $(\bar{1}01)$ plane. In particular, this occurred for tension in the [012] and $[\bar{2}38]$ directions and compression in the $[\bar{1}11]$ direction. A typical example of the core changes that took place just prior to the onset of the motion along the $(\bar{1}01)$ plane is shown in figure 11 for the case of tension in the $[\bar{2}38]$ direction. Comparison with figure 7 (*b*) shows that the shift of the centre of the dislocation that signals the motion along $(\bar{1}\bar{1}2)$ in the twinning sense does not occur. Instead, the dislocation remains in the configuration similar to that seen in figure 7 (*a*) and starts to move along the $(\bar{1}01)$ plane. However, neither the analysis of the changes in the dislocation core induced by tension and compression nor the dependences of the CRSS on the orientation of the tension or compression axes provide sufficient information for the full understanding of the effect of stress components other than $\tau_{\parallel}$ on the motion of $\frac{1}{2}[111]$ screw dislocations.

The most comprehensive investigation of the effect of these stress components on the core structure and glide of $\frac{1}{2}[111]$ screw dislocations was performed by Duesbery (1984a, b). These calculations were done by applying combinations of stresses in an atomistic model employing pair potentials for K (Dagens *et al.* 1975) and Fe (Johnson 1964). Among possible components of the stress tensor other than $\tau_{\parallel}$, only shear stresses in the direction perpendicular to the Burgers vector were found to have a significant influence. In the following we denote these stresses as $\tau_{\perp}$. In the dependence on the orientation of the plane in which $\tau_{\perp}$ was a maximum, its effect varied from the total locking of the dislocation to decreasing the glide stress needed for its motion (the Peierls stress) to almost zero. The effect of other stress tensor components, such as tension (compression) normal to the glide plane, was found to be negligible. The combined effect of $\tau_{\parallel}$ and $\tau_{\perp}$ on the motion of $\frac{1}{2}[111]$ screw dislocations is investigated in the following section.

4.3. *Combination of shear stresses parallel and perpendicular to the Burgers vector*

In order to decipher the orientation dependence of the influence of shear stresses perpendicular to the Burgers vector, $\tau_{\perp}$, on dislocation glide, we have to think about

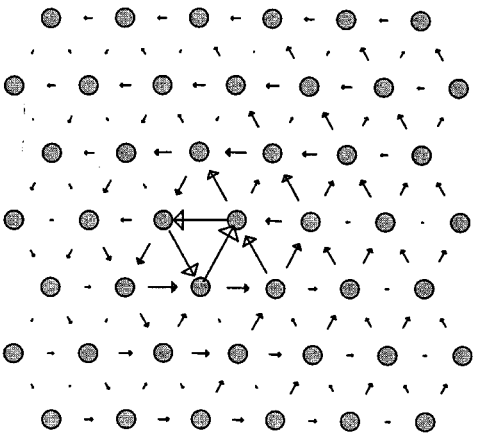

Figure 11. The displacement map of the dislocation core in Ta just prior to the onset of the motion along the $(\bar{1}01)$ plane for the case of tension in $[\bar{2}38]$ direction.

the possible origin of this effect in the dislocation core structure. As shown in figures 2(*b*) and 3(*b*), there are edge components within the core of the screw dislocation. The shear stress in the direction perpendicular to the total Burgers exerts a Peach–Koehler force on these components while it produces no total force on the screw dislocation. It is, therefore, feasible that the response to $\boldsymbol{\tau}_\perp$ is mediated through these edge components. This is analogous to the influence of shear stresses in the direction perpendicular to the total Burgers upon the cross-slip in fcc materials, as first suggested by Escaig (1968, 1974) and Bonneville *et al.* (1988). This effect arises owing to the forces that these stresses exert on the edge components of the Shockley partials into which the $\frac{1}{2}\langle 110\rangle$ screw dislocation dissociates.

Since the core of the $\frac{1}{2}\langle 111\rangle$ screw dislocation in bcc crystals is spread predominantly into {110} planes of the corresponding $\langle 111\rangle$ zone, it is natural to consider shear stresses perpendicular to the total Burgers acting in these planes. One such study was performed by Duesbery and Vitek (1998) where a pure shear stress acting in the $(\bar{1}01)$ plane in the $[\bar{1}2\bar{1}]$ direction was applied to a block containing a $\frac{1}{2}[111]$ screw dislocation. Very significant changes in the core structure were induced by this stress, particularly in metals with the core structure of the same type as Mo. However, this result cannot be directly related to studies of tension and compression. For example, in the case of $[\bar{2}38]$ and [012] axes, when $(\bar{1}01)$ is the MRSSP, this stress component vanishes although shear stresses perpendicular to the total Burgers vector are present in other planes of the [111] zone.

Hence, to investigate the influence of shear stresses perpendicular to the total Burgers vector in a manner useful for understanding tension and compression, we have to inspect first what shear stresses of this type are induced in the case of uniaxial loading. Considering planes of {110} type, the three planes and directions in which these stresses need to be examined are as follows: $(\bar{1}01), [\bar{1}2\bar{1}]$; $(\bar{1}10), [11\bar{2}]$; $(0\bar{1}1), [\bar{2}11]$. If α is the angle between the tensile or compressive axis and the normal to the corresponding {110} plane, and β is the angle between this axis and the direction of shear, the corresponding shear stress perpendicular to the total Burgers vector is $\tau_{\{110\}} = \sigma \cos\alpha \cos\beta$, where σ is the applied tensile or compressive stress. For axes $[\bar{2}38]$ and [012], $\tau_{(\bar{1}01)} = 0$ and $\tau_{(\bar{1}10)} = -\tau_{(0\bar{1}1)}$; $\tau_{(0\bar{1}1)}$ is positive for tension. For axes $[\bar{1}11], [\bar{1}22]$ and [011], $\tau_{(0\bar{1}1)} = 0$ and $\tau_{(\bar{1}10)} = -\tau_{(\bar{1}01)}$ and, for the axis [001], $\tau_{(\bar{1}10)} = 0$ and $\tau_{(0\bar{1}1)} = -\tau_{(\bar{1}01)}$; $\tau_{(\bar{1}01)}$ is positive for tension in both cases. Using these results as a guideline, we always apply such shear stresses perpendicular to the total Burgers vector that we can attain the above values of $\tau_{\{110\}}$ on chosen {110} planes. For a given MRSSP, characterized by the angle χ, this is achieved by applying the stress tensor

$$\boldsymbol{\tau}_\perp = \begin{pmatrix} -\tau & 0 & 0 \\ 0 & \tau & 0 \\ 0 & 0 & 0 \end{pmatrix} \tag{1}$$

in the right-handed coordinate system with the x_1 axis in the MRSSP, the x_2 axis perpendicular to the MRSSP and the x_3 axis parallel to [111]. It is important to note that changing the sign of $\boldsymbol{\tau}_\perp$ corresponds to the coordinate transformation obtained from a rotation by 180° around the [111] axis. However, the core structure is not invariant with respect to this transformation and thus the effect of $\boldsymbol{\tau}_\perp$ upon the core behaviour can be expected to be different for positive and negative values of τ. This is, indeed, shown in the calculations presented below.

The study of the effect of shear stresses perpendicular to the total Burgers vector on the CRSS proceeded as follows. First the MRSSP in which $\tau_{\parallel}$ will be applied was chosen. In the next step $\tau_{\perp}$, given by equation (1), was applied and the structure relaxed. Finally, similarly to the study of the effect of the pure shear stress (§4.1), $\tau_{\parallel}$ was applied and gradually increased until the dislocation started to move. In this way, for a chosen MRSSP, we obtained the dependence of the CRSS on τ. The calculations were carried out for the MRSSPs taken as $(\bar{1}01)$, $(\bar{1}\bar{1}2)$ and $(\bar{2}11)$. $\tau_{\parallel}$ was always applied such that the dislocation moved to the right when considering figures 2 and 3, so that the $(\bar{1}\bar{1}2)$ plane was sheared in the twinning and $(\bar{2}11)$ in the antitwinning sense. The results are shown in figures 12 and 13 for Mo and Ta respectively.

The values of the CRSS for tensions and compressions described in §4.2 are also displayed in figures 12 and 13; for each uniaxial loading the value of τ is uniquely

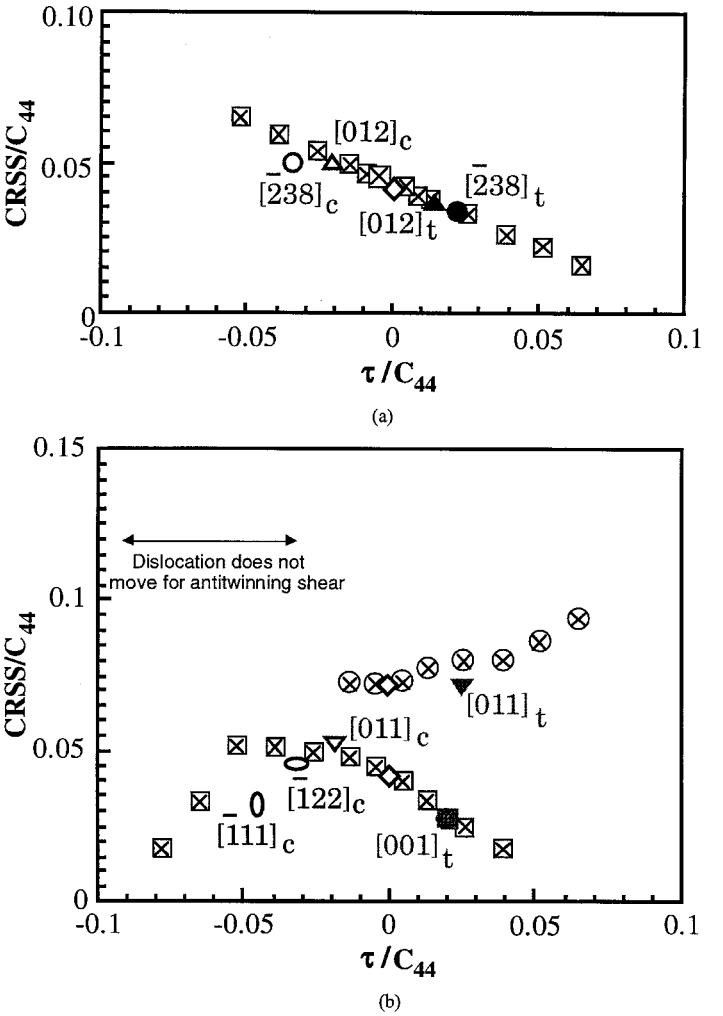

Figure 12. Dependence of the CRSS on τ in Mo: (*a*) MRSSP is the $(\bar{1}01)$ plane; (*b*) MRSSP is the $(\bar{1}\bar{1}2)$ plane sheared in the twinning sense (□) and $(\bar{2}11)$ plane sheared in the antitwinning sense (⊗).

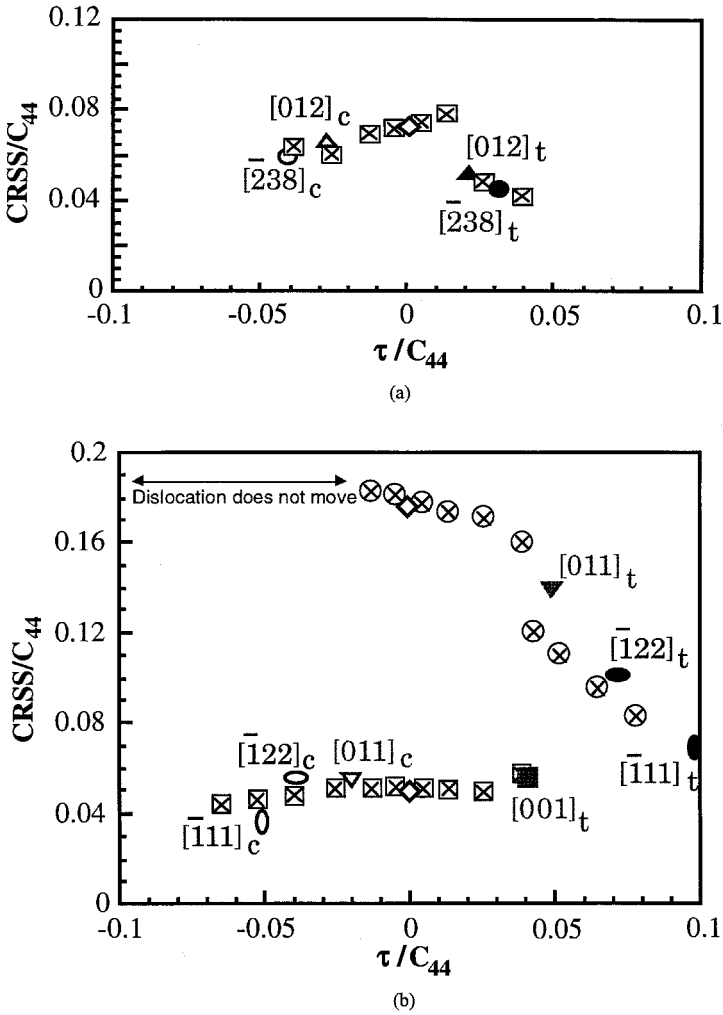

Figure 13. Dependence of the CRSS on τ in Ta: (*a*) MRSSP is the $(\bar{1}01)$ plane; (*b*) MRSSP is the $(\bar{1}\bar{1}2)$ plane sheared in the twinning sense (□) and $(\bar{2}11)$ plane sheared in the antitwinning sense (⊗).

related to the loading stress, and thus to the CRSS, by the corresponding tensor transformation. This comparison clearly demonstrates that the variation in the CRSS found for uniaxial loadings, with the MRSSP and the sense of glide shearing fixed, is governed by the shear stresses in the direction perpendicular to the Burgers vector that are represented by the deviatoric stress tensor given by equation (1). The results also demonstrate the 'asymmetry' mentioned above, namely that the positive and negative values of τ lead to different magnitudes of CRSS. This feature is further corroborated by figure 14, which shows the core structures of the screw dislocation in Mo under the effect of only $\tau_\perp$ when $\tau = \pm 0.052 C_{44}$, and the MRSSP, determining the coordinate system for $\tau_\perp$, is the $(\bar{1}01)$ plane. For $\tau < 0$ the branch in the $(0\bar{1}1)$ plane extends significantly more than does the branch in the $(\bar{1}10)$ plane for $\tau > 0$. As a result, the branch in the $(\bar{1}01)$ plane contracts for $\tau < 0$ but remains almost

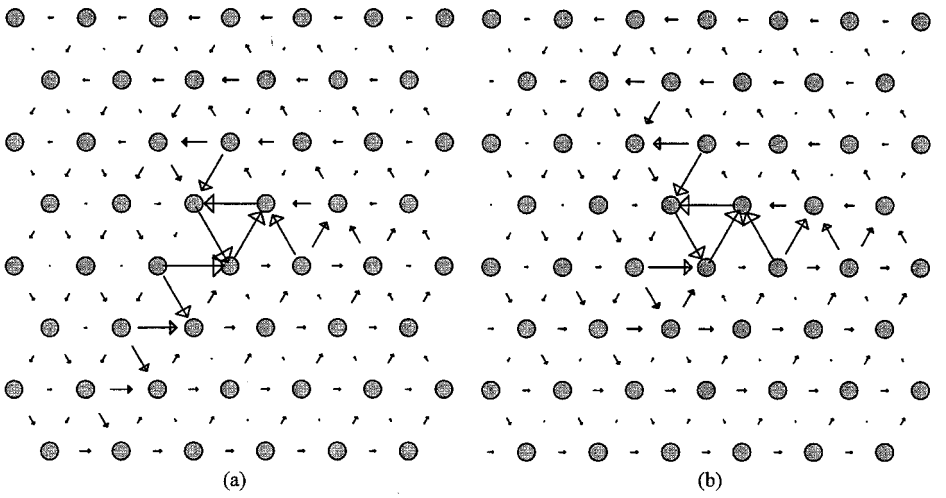

Figure 14. The displacement maps of the dislocation core in Mo under the effect of $\tau_\perp$ given by equation (1) when (*a*) $\tau = -0.052C_{44}$ and (*b*) $\tau = +0.052C_{44}$.

unaffected for $\tau > 0$. Consequently, the CRSS is higher for $\tau < 0$ than for $\tau > 0$ when the magnitude of τ is the same.

Finally, an important observation is that the effects of $\tau_\perp$ are both quantitatively and qualitatively different for Mo and Ta. This is in contrast with the effects of $\tau_\parallel$, which display qualitatively the same features even though the twinning–antitwinning asymmetry of the CRSS in pure shear is more pronounced in Ta than in Mo (cf. figures 5 (*a*) and (*b*)). This difference is, presumably, related to very different components of the displacements perpendicular to the Burgers vector inside the core in the two cases (cf. figures 2 (*b*) and 3 (*b*)).

§ 5. Discussion

In this paper we have investigated by computer modelling the response of the core of $\frac{1}{2}[111]$ screw dislocations that control the plastic behaviour of bcc metals, to externally applied stresses. The calculations, employing central-force many-body potentials (Ackland and Thetford 1987), were made for two distinct nonplanar forms of core structures that have been found in previous calculations (Duesbery and Vitek 1998) and are here associated with Mo and Ta respectively. In the latter case the core structure is unique (figure 3) while in the former case there are two symmetry-related variants (figure 2). However, when applying the stress, only that variant which is easier to move need to be considered since, as discussed in § 3, we may assume that both configurations of the core are always present along the dislocation line and the configuration that moves more easily determines the CRSS for dislocation glide.

All calculations in this study correspond to 0 K and the effect of temperature upon the CRSS has not been examined. Still, the stresses at which the dislocation motion commences are considerably higher than the values of the CRSS determined from low-temperature experiments by extrapolation towards 0 K. This is characteristic for many atomistic studies of dislocation motion as discussed, for example, by Duesbery (1989). The reason for this discrepancy is still not clear but possibilities are

adiabatic heating that lowers the observed CRSS at very low temperatures, zero vibrations that are of quantum origin and not included in classical calculations, or simply inapt extrapolations from accessible low-temperature data to 0 K. However, the principal goal of this study has not been to evaluate the magnitude of the CRSS but to examine the breakdown of the Schmid law and to establish, as a result, the dependence of the CRSS in the MRSSP in the slip direction upon the applied stress tensor. This important aspect of the dislocation behaviour depends principally on relative values of the CRSS for differently applied loads and the absolute magnitude of the CRSS is of secondary importance.

In the first part of this study, only the shear stress parallel to the Burgers vector, that is, the stress which exerts the Peach–Koehler force on the $\frac{1}{2}[111]$ screw dislocation, was applied. The MRSSP was characterized by the angle χ, as defined in § 4.1 (see figure 4). The slip plane, defined as the plane along which the dislocation moves when the CRSS has been reached, was found to be the $(\bar{1}01)$ plane ($\chi = 0$) in the case of Mo but the $(\bar{1}\bar{1}2)$ plane ($\chi = -30^\circ$) that is sheared in the twinning sense in the case of Ta. While the slip planes are different in the two cases, the dependence of the CRSS on χ displays similar characteristics for both Mo and Ta. In both cases the CRSS does not obey the Schmid law and the deviation increases as the MRSSP approaches the $(\bar{2}11)$ plane sheared in the antitwinning sense ($\chi = +30^\circ$). This is the origin of the well known twinning–antitwinning asymmetry of slip in bcc metals. This asymmetry is significantly stronger in Ta than in Mo although the unstressed core displays a higher symmetry in Ta than in Mo. In fact, in the case of Ta the CRSS reaches the ideal strength for shear on {112} when the MRSSP is the {112} plane sheared in the antitwinning sense ($\chi = +30^\circ$). This demonstrates that the transformations of the core induced by the applied stress prior to the dislocation motion are the controlling factor in the choice of the slip plane and in the orientation dependence of the CRSS. As discussed in more detail in § 4.1, shear stresses acting in the [111] direction in all three {110} planes containing this direction are responsible for the core changes. However, it should be noted that these changes cannot be discerned directly from the structure of the unstressed core and are only revealed by studying the influence of externally applied stresses on the dislocation cores and eventual dislocation glide.

The next step in this study has been exploration of the effect of tensile and compressive stresses on the motion of screw dislocations. These calculations, performed for five distinct orientations of the tension or compression axes (figure 8), demonstrate that differences in shear stresses parallel to the Burgers vector are not sufficient to explain the variation in the CRSS with the orientation of the loading axis. This implies that other components of the stress tensor are affecting the dislocation behaviour. This effect is particularly strong when the MRSSP is a {112} plane sheared in the antitwinning sense since all the stress components are very high owing to the high shear stress $\tau_{\parallel}$ needed for the dislocation motion.

In order to unravel the dependence of the CRSS on other components of the stress tensor than $\tau_{\parallel}$ we investigated the combined effect of $\tau_{\parallel}$ and the shear stresses $\tau_{\perp}$ perpendicular to the Burgers vector. The reason why other stress components have not been considered is that an earlier study by Duesbery (1984a, b) demonstrated that among all possible components of the stress tensor other than $\tau_{\parallel}$ only $\tau_{\perp}$ has a significant influence. $\tau_{\perp}$ was taken in the form given by equation (1) in order to link this investigation with studies of tension and compression. These calculations clearly demonstrate the effect of $\tau_{\perp}$ on the glide of the $\frac{1}{2}[111]$ screw dislocation and

explain the orientation dependence of the CRSS found when applying tensile and compressive stresses. This effect can be interpreted as induced by the force exerted by $\tau_\perp$ on the edge components of fractional dislocations describing the core spreading and is analogous to the influence of stresses perpendicular to the total Burgers upon the cross-slip in fcc materials (Escaig 1968, 1974, Bonneville *et al*. 1988). This immediately explains why the effects of $\tau_\perp$ are both quantitatively and qualitatively different for Mo and Ta although the effects of $\tau_\parallel$ are qualitatively the same in both cases. As seen in figures 2 (*b*) and 3 (*b*), the edge components inside the core are very different in the two cases. As discussed in § 4.3, it follows from the asymmetry of the core that $\tau_\perp$ will affect the core behaviour differently for positive and negative values of τ. When interpreting this asymmetry through the forces exerted on the edge components of fractional dislocations, it implies that it is not only the shear stress perpendicular to the Burgers vector acting in {110} planes but also the corresponding shear stress acting in {112} planes that influence the core transformations occurring prior to the dislocation motion and thus the CRSS.

In conclusion, the present atomistic calculations establish that gliding of the $\frac{1}{2}$[111] screw dislocation in bcc metals depends on shear stresses both parallel and perpendicular to the Burgers vector that act not only on the slip plane but also in all three {110} and {112} planes of the [111] zone. Furthermore, the results determine the functional dependences of the CRSS on these shear stresses and these can be employed in a full three-dimensional continuum theory of multiple slip in bcc crystals. Such studies are at present in progress and preliminary results have been presented by Bassani *et al*. (2001).

Acknowledgements

This research was supported by the Advanced Strategic Computing Initiative of the US Department of Energy through Lawrence Livermore National Laboratory (grant B501663) and by the National Science Foundation (grant CMS99-00131). K. Ito would like to acknowledge the Japan Society for the Promotion of Science Postdoctoral Fellowship for Research Abroad.

References

Ackland, G. J., and Thetford R., 1987, *Phil. Mag.* A, **56**, 15.
Asaro, R. J., 1983, *Adv. appl. Mech.*, **23**, 1.
Basinski, Z. S., Duesbery, M. S., and Murthy, G. S., 1981, *Acta metall.*, **29**, 801.
Basinski, Z. S., Duesbery, M. S., and Taylor, R., 1971, *Can. J. Phys.*, **49**, 2160; 1972, *Interatomic Potentials and Simulation of Lattice Defects*, edited by P. C. Gehlen, J. R. Beeler R. I. Jaffee (New York: Plenum), p. 537.
Bassani, J. L., 1994, *Adv. appl. Mech.*, **30**, 191.
Bassani, J. L., Ito, K., and Vitek, V., 2001, *Mater. Sci. Engng.* A (to be published).
Bonneville, J., Escaig, B., and Martin, J. L., 1988, *Acta metall.*, **36**, 1989.
Christian, J. W., 1970, *Proceedings of the Second International Conference on the Strength of Metals and Alloys*, edited by W. C. Leslie (Metals Park, Ohio: American Society for Metals), p. 31; 1983, *Metall. Trans.* A, **14**, 1237.
Dagens, K., Rasolt, L. M., and Taylor, R., 1975, *Phys. Rev.* B, **11**, 2726.
Duesbery, M. S., 1969, *Phil. Mag.*, **19**, 501; 1984a, *Proc. R. Soc.* A, **392**, 145; 1984b, *ibid.*, **392**, 175; 1989, *Dislocations in Solids*, Vol. 8, edited by F. R. N. Nabarro (Amsterdam: North-Holland), p. 67.
Duesbery, M. S., and Foxall, R. A., 1969, *Phil. Mag.* A, **20**, 719.
Duesbery, M. S., and Hirsch, P. B., 1968, *Dislocation Dynamics*, edited by G. T. Hahn, A. L. Bement and R. I. Jafee (New York: McGraw-Hill), p. 57.
Duesbery, M. S., and Vitek, V., 1998, *Acta mater.*, **46**, 1481.

Duesbery, M. S., Vitek, V., and Bowen, D. K., 1973, *Proc. R. Soc.* A, **332**, 85.
Escaig, B., 1968, *J. Phys., Paris*, **29**, 225; 1974, *ibid.*, **35**, C7–151.
Finnis, M. W., and Sinclair, J. E., 1984, *Phil. Mag.* A, **50**, 45.
Foxall, R. A., Duesbery, M. S., Hirsch, P. B., 1967, *Can. J. Phys.*, **45**, 607.
Friedel, J., 1969, *The Physics of Metals*, edited by J. M. Ziman (Cambridge University Press), p. 340.
Hill, R., and Rice, J. R., 1972, *J. Mech. Phys. Solids*, **20**, 401.
Hirsch, P. B., 1960, *Proceedings of the Fifth International Conference on Crystallography* (Cambridge University Press), p. 139.
Hirth, J. P., and Lothe, J., 1982, *Theory of Dislocations* (New York: Wiley–Interscience).
IsmailBeigi, S., and Arias, T. A., 2000, *Phys. Rev. Lett.*, **84**, 1499.
Johnson, R. A., 1964, *Phys. Rev.* A, **134**, 1329.
Kroupa, F., 1963, *Phys. Stat. Sol.* (a), **3**, K391.
Kubin, L. P., 1982, *Rev. Deformation Behaviour Mater.*, **4**, 181.
Kuramoto, E., Minami, F., and Takeuchi, S., 1974, *Phys. Stat. Sol.* (a), **22**, 411.
Masuda, K., and Sato, A., 1978, *Phil. Mag.* B, **37**, 531.
Minami, F., Kuramoto, E., and Takeuchi, S., 1972, *Phys. Stat. Sol.* (a), **12**, 581; 1974, *ibid.*, **22**, 81.
Moriarty, J. A., 1990a, *Phys. Rev.* B, **42**, 1609; 1990b, *Many-Atom Interactions in Solids*, Vol. 48, edited by R. M. Nieminen, M. J. Puska and M. J. Manninen (Berlin: Springer), p. 158.
Neumann, F., 1885, *Vorlesungen über die Theorie der Elasticität* (Leipzig).
Pettifor, D. G., 1995, *Bonding and Structure of Molecules and Solids* (Oxford University Press).
Qin, Q., and Bassani, J. L., 1992a, *J. Mech. Phys. Solids*, **40**, 835; 1992b, *ibid.*, **40**, 813.
Rice, J. R., 1971, *J. Mech. Phys. Solids*, **19**, 433.
Sato, A. and Masuda, K., 1981, *Phil. Mag.* B, **43**, 1.
Schmid, E., and Boas, W., 1935, *Kristallplastizität* (Berlin: Springer).
Taylor, G., 1992, *Prog. Mater. Sci.*, **36**, 29.
Taylor, G. I., 1928, *Proc. R. Soc.* A, **118**, 1.
Taylor, G. I., and Elam, C. F., 1926, *Proc. R. Soc.* A, **112**, 337.
Vitek, V., 1968, *Phil. Mag.* A, **18**, 773; 1975, *Cryst. Lattice Defects*, **5**, 1; 1985, *Dislocations and Properties of Real Materials*, edited by M. Lorretto (London: Institute of Metals) p. 30; 1992, *Prog. Mater. Sci.*, **36**, 1.
Vitek, V., and Duesbery, M. S., 1982, *Mechanical Properties of BCC Metals*, edited by M. Meshii (Warrendale, Pennsylvania: Metallurgical Society of AIME), p. 3.
Vitek, V., Perrin, R. C., and Bowen, D. K., 1970, *Phil. Mag.* A, **21**, 1049.
Vitek, V., Pope, D. P., and Bassani, J. L., 1996, *Dislocations in Solids*, Vol. 10, edited by F. R. N. Nabarro and M. S. Duesbery (Amsterdam: Elsevier), p. 135.
Woodward, C., and Rao, S. I., 2001, *Phil Mag.* A, **81**, 1305.
Xu, W., and Moriarty, J. A., 1996, *Phys. Rev.* B, **54**, 6941.
Yang, L. H., Söderlind, P., and Moriarty, J. A., 2001, *Phil. Mag.* A, **81**, 1355.